COMMUNICATION

Direct Laser Writing of Photoresponsive Colloids for Microscale Patterning of 3D Porous Structures

By *Matthew C. George, Ali Mohraz, Martin Piech, Nelson S. Bell, Jennifer A. Lewis,* and *Paul V. Braun**

Several routes have recently been introduced for microscale patterning of materials in three dimensions, including multilayer photolithography,[1–3] nanotransfer printing,[4] LiGA, a german acronym for Lithographie–Galvanoformung–Abformung (lithography-electroplating-molding),[5] microstereolithography,[5,6] and multiphoton polymerization.[7] Each of these routes typically yields a solid structure,[8] yet novel porous architectures such as those assembled from colloidal building blocks, are required for applications ranging from microfluidic filters and mixing elements to catalyst supports.[9–12] Direct-write assembly of colloidal inks offers a pathway for creating the desired porous structures. However, their minimum dimensions must exceed 100 μm to maintain continuous ink flow during deposition.[13,14] To overcome this limitation, we harness the power of multiphoton direct laser writing to locally define the interactions between photoswitchable colloidal microspheres suspended in an organic solvent. Through this novel approach, we create porous-walled 3D structures including microscale rectangular cavities that exhibit size-selective permeability.

Direct laser writing of photoresponsive colloids consists of three basic steps (see Fig. 1a–c). First, we produce a dense colloidal suspension via sedimentation of a dilute solution of photoresponsive microspheres (Fig. 1a). Next, we locally induce colloidal gelation by photoswitching these microspheres from a repulsive to an attractive state (Fig. 1b). We achieve this transformation by rastering a high-intensity near-IR pulsed laser that alters the polymer brush chemistry, and hence colloidal stability, via a two-photon absorption process. Finally, we remove the unexposed microspheres through a simple rinsing step, leaving behind the desired 3D structure (Fig. 1c).

[*] Prof. P. V. Braun, M. C. George, Prof. A. Mohraz,[+] Prof. J. A. Lewis
Department of Materials Science and Engineering
Frederick Seitz Materials Research Laboratory
Beckman Institute
University of Illinois at Urbana-Champaign
Urbana, IL 61801 (USA)
E-mail: pbraun@uiuc.edu
Dr. M. Piech,[++] Dr. N. S. Bell
Electronic and Nanostructured Materials
Sandia National Laboratories, P.O. Box 5800-1411
Albuquerque, New Mexico 87185 (USA)
Prof. A. Mohraz
[+] Present Address: Department of Chemical Engineering and Materials Science, University of California, Irvine, CA, USA
Dr. M. Piech
[++] Present Address: United Technologies Research Center, East Hartford, CT 06108, USA

DOI: 10.1002/adma.200801118

The photoresponsive microspheres are formed by grafting a copolymer brush 55 nm thick (dry thickness) onto silica colloids with 927 nm diameter (Fig. 1d). The brush layer is grown using surface-initiated atom-transfer radical polymerization (ATRP), and is composed of methyl methacrylate (MMA) containing 20% spirobenzopyran (SP) pendant groups poly(SP-*co*-MMA), as shown in Figure 1e. In the SP-form, the microspheres are sterically stabilized when suspended in a nonpolar solvent such as toluene. However, upon irradiation with UV or high-intensity near-IR pulsed radiation (utilizing two-photon absorption), the SP side groups photoisomerize into the polar, zwitterionic merocyanine (MC) form (see Fig. 1f). In toluene, the exposed colloids, now coated with the MC-rich form of the copolymer, undergo rapid flocculation when they come into contact via Brownian motion.[15–17] It has been postulated that MC–MMA, MC–SP, and H-stacked MC–MC aggregates are all present, and contribute to the strong intermolecular and interparticle bonding in this system.[16,17] While the reverse reaction back to the sterically stabilized SP-form can be induced upon exposure to visible wavelengths ($\lambda_{max} = 585$ nm), the colloidal microspheres remain flocculated, and significant mechanical agitation is required to break up the particle network.

Figure 2 depicts two simple structures fabricated using direct laser writing that illustrate the power of this approach. The ''MRL'' structure is composed of high-aspect-ratio walls (Fig. 2a–c), and the ''mushrooms'' are examples of complex 3D self-supporting features (Fig. 2d–i). Spatially defined colloidal gelation is phototriggered by scanning a focused, pulsed Ti/Sapphire laser through a dense sediment of photoresponsive microspheres in toluene. The flux is only sufficient for two-photon triggered photoisomerization within the focal volume. Thus, photoswitching of the SP side groups into their MC form occurs solely in these highly illuminated regions within the sediment. The substrate is also derivatized with the poly(SP-*co*-MMA) brush, and locally photoswitched to prevent delamination, based on our previous work where we demonstrated multiphoton directed adhesion of colloidal particles to planar substrates.[17] The bright areas of Figure 2a and d, and the four large discs with dark centers of Figure 2g are regions exposed via direct laser writing, and contain aggregated microspheres coated with the MC-form of the polymer brush. The microspheres in the unexposed regions (backgrounds of Fig. 2a, d, and g), remain in the nonaggregating SP-form and can be removed simply by rinsing in toluene to give the desired microstructure (Fig. 2b, e, and h). 3D renderings of the MRL and mushrooms structures are provided in Figure 2c, f, and i.

By integrating both high aspect ratio and self-supporting features, we can produce the 3D microcavity shown in Figure 3.

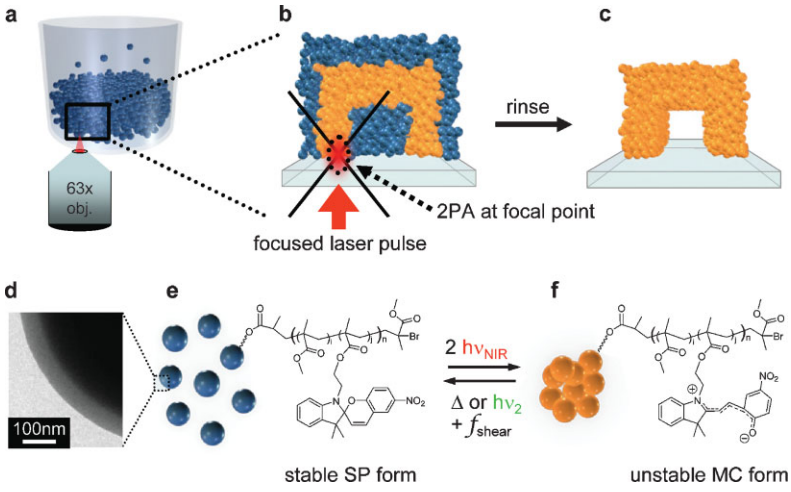

Figure 1. Schematic view of direct laser writing with photoresponsive colloidal microspheres (a–c), and their architecture and reversible phototriggered aggregation (d–f). a) A dense colloidal suspension is formed via sedimentation of the photoresponsive colloids onto a modified silica substrate. b) Magnified view of the patterning process, which shows localized colloidal gelation induced by two-photon absorption (2 PA) at the focal point of a near-IR pulsed laser. c) 3D structure composed of porous walls is harvested after rinsing away unexposed colloidal species. d) TEM image of the photoresponsive microspheres' core/shell architecture showing the silica core and the SP-*co*-MMA polymer-brush layer (or shell). Forward ring-opening reaction from (e) closed-form SP to (f) zwitterionic MC isomer is facilitated by two-photon near-IR excitation. The reverse reaction is accelerated by heat or single photon visible excitation. The copolymer contains 20 mol % of the SP/MC monomer unit ($i = 80\%$, $j = 20\%$).

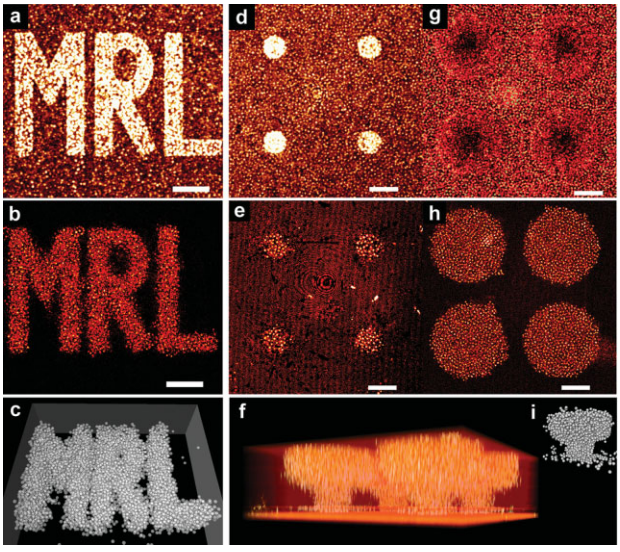

Figure 2. Reflectance-mode confocal microscopy images of direct laser writing fabrication process and corresponding 3D reconstructions of patterned structures. a–c) High aspect ratio structure. d–i) Self-supported mushroom structures. Confocal *x*–*y* sections taken (d,e) through the mushroom stem, $<1\,\mu m$ above the substrate, and (g, h) through the cap of the mushroom, $\sim 14\,\mu m$ above the substrate. Frames in the top row are in situ reflectance-mode images taken during direct laser writing in a dense sediment of photoresponsive colloids. Photoswitched colloidal gel regions have enhanced reflectivity and appear as bright areas when imaged near the substrate (a,d). Further away from the substrate, the contrast is reduced (g). Frames in the middle row are reflectance-mode images revealing the patterned gel structures after rinsing. The bottom row contains the corresponding 3D reconstructions. All scale bars = 10 μm.

Effective rinsing requires a continuous path for the stable, SP-form colloidal species to escape, thus this structure is formed through a series of steps. First, an open-ended microtube with vertical side walls is constructed, as depicted in Figure 3a–c. The side walls are approximately 10 μm thick and 20 μm tall, and are capped with a gelled colloidal layer approximately 10 μm thick, that spans across the channel yielding a hollow rectangular tube after removal of the unexposed colloids. The efficiency of the rinsing process is revealed in Figure 3a and b; nonpatterned (stable) colloidal species are almost completely removed in this step. The resulting 3D microtube is composed of porous walls, whose pore structure closely matches that of the dense colloidal sediment from which they are formed. Next, the ends of the tube are sealed by introducing a dilute solution of photoresponsive colloids over the as-patterned structure. As they sediment, the laser is rastered to dynamically "fuse" the colloidal species to one another and to the already-present structure, locking them into place before they have time to diffuse into the interior of the cavity. Although it is not possible to write free standing structures in a dynamic fashion (e.g., the top of a channel before its supporting side walls are constructed), this approach does enable the formation of capping walls at each end of the rectangular microcavity (see Fig. 3d and e). To prevent damage from capillary drying stresses that result in structural collapse, the as-patterned structures remain immersed in solution during the entire fabrication process.

As revealed by the laser scanning confocal microscopy (LSCM) images in Figure 2a, 2d, 3a, and 3d the photoresponsive colloidal species exhibit a marked change in reflectivity after being photoswitched from the SP- to the MC-form via direct laser writing. Reflectance-mode image contrast arises due to the pronounced photochromic and photophysical changes that occur in the SP/MMA copolymer brush upon conversion to the MC-form in toluene, including changes in index of refraction,[18] absorption coefficient,[15] and polymer-brush conformation.[19] The confocal image shown in Figure 4a, acquired in fluorescence mode, depicts a section through an end-capped 3D cavity structure after transfer into ethanol. In this case, contrast is derived from the fact that the trans-MC-form is significantly more fluorescent in glassy media (like the MMA-rich polymer brush in ethanol), than the SP-form.[20–22]

The porous nature of the patterned rectangular microcavity is demonstrated by introducing a fluorescent dye into the surrounding fluid, which diffuses into the interior of the cavity. LSCM images acquired in fluorescence mode show that the cavity interior and surrounding regions outside of the porous structure are initially dark (Fig. 4a), but then become uniformly bright upon addition of the dye (Fig. 4b). The size exclusivity is evident in Figure 4c and d. In Figure 4c, 490 nm silica colloids have been introduced into the sedimentation cell, but the photopatterned gel walls prevent them from filling the central cavity. To resolve the 490 nm colloids, this confocal image (*x*–*y* scan) was taken at the base of the cavity, just above the coverslip. Away from the

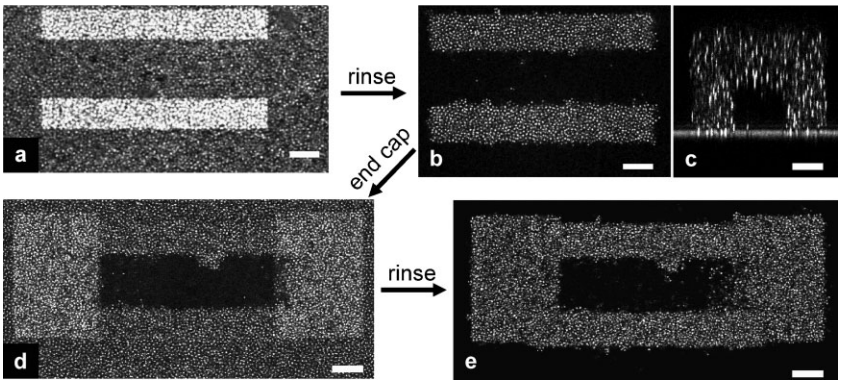

Figure 3. Reflectance-mode confocal microscopy images of fabrication process for a capped, porous-walled 3D microtube. a) In situ *x*–*y* scan of direct laser writing of microtube sidewalls in a dense sediment of photoresponsive colloids (photoswitched colloids appear as bright features). b,c) Confocal images of patterned 3D microtube after rinsing. b) An *x*–*y* section taken mid-channel while (c) is a cross-section view (*x*–*z* scan). d,e) Confocal *x*–*y* sections of an end-capped microtube taken before rinsing (d) and after rinsing (e). All scale bars = 10 μm.

substrate, the 490 nm colloids are moving rapidly, and are difficult to image; they are best observed in the LSCM movie taken mid-channel (movie S1 of Supporting Information). In Figure 4c, the 1 μm colloids observed both inside and outside the cavity are physisorbed to the substrate, and were not removed by the rinsing step. If the end-caps are not rapidly patterned during the second sedimentation step, one arrives at Figure 4d, in which a colloidal fluid of nonswitched poly(SP-*co*-MMA)-coated silica particles fills the microcontainer. In this image, the stationary colloids are shown in grayscale, and the particles in motion are depicted in red. A second LSCM movie (movie S2 of Supporting Information), clearly displays the trapped colloidal fluid rapidly undergoing Brownian and convective motion inside the capped microtube. The structures depicted are robust and can survive solvent transfer from toluene into THF, ethanol, and water. If left in THF or toluene for long periods of time with agitation, the structures break apart, presumably as the MC isomer reverts to the SP-form; with vigorous agitation, the structures can be completely erased. For example, we regenerate the polymer-brush-coated substrates by ultrasonication in toluene and THF. The photoresponsive microspheres can also be harvested and reused.

Direct laser writing of photoresponsive colloidal species enables one to pattern 3D structures of near arbitrary geometry with controlled feature size, roughness, and porosity. To demonstrate this, we created structures with a nominal feature size of 10 μm, more than an order of magnitude finer than those produced by direct ink writing of colloidal microspheres.[13] The minimum feature size possible through this approach appeared to be ~5 μm (see Fig. S1 of Supporting Information), and is determined by several factors, including Brownian motion during the writing step, two-photon excitation volume, colloid diameter, and processing limitations. By writing into a dense sediment, Brownian diffusion is significantly suppressed, and thus does not limit resolution. In our system, the positional accuracy of the focal point is ~58 nm, and the size of the intensity-squared point spread function is ~390 nm in plane and 1.5 μm out of plane,[23] implying the multiphoton excitation step is also not a limiting factor. We previously found the sticking coefficient to be unity for unexposed SP colloids on a MC surface,[17] thus unexposed SP-form colloids will form a passivating monolayer around any photodefined gel structure. When this is coupled with the surface roughness of the gel walls due to random colloid placement, the minimum channel-design width is 4 colloid diameters (~4 μm in our system). Nonswitched colloids cannot be removed from channels narrower than this size. In addition, it appears that channel walls thinner than ~5 μm are not mechanically stable to removal of the nonswitched colloidal sediment. By tailoring the colloid diameter and sticking coefficient, it may be possible to create finer patterned features, and strongly influence the resulting pore morphology. We imagine that it will be possible to further tune permeability and size exclusivity by introducing other colloidal species of varying size and concentration that are either reactive or inert.

In summary, we have introduced a new route for patterning 3D porous structures at the microscale by coupling direct laser writing with photoresponsive colloidal building blocks. These locally defined architectures may find potential application as functional elements (e.g., chaotic mixers and filters) in microfluidic devices. Permeable microcontainers have also found uses including bacteria sequestration and incubation.[24] Given their photoreversible nature, there is great potential for dynamic control of element geometry, permeability, and size selectivity via programmable assembly and disassembly of the colloidal building blocks or simply by photoactuation of the polymer-brush conformation.[19] In addition, this approach allows one to construct model systems for studying the dynamics of confined colloidal fluids, flow through porous media, and colloidal gelation.

Experimental

Materials and Instruments: 927 nm diameter SiO_2 colloids were obtained from Fuso Chemical Co., Ltd. (grade SP-1B) and used without further purification. Substrates employed were 1 in sq. fused-silica coverslips (0.0197 ± 0.002 in thick) from Valley Design. These silica colloids and substrates were derivatized with SP-*co*-MMA polymer brushes containing 20% SP pendant groups via surface initiated ATRP. For detailed synthetic conditions see previous work [15,17]. The TEM image (Fig. 1d) was obtained on a Philips CM30 TEM/STEM operating at 300 kV using the SP-1B grade silica spheres with 55 nm thick SP-*co*-MMA shells. A custom sedimentation cell was used for the direct laser writing experiments with an SP-*co*-MMA coated coverslip base, Viton O-ring sides, and Delrin top containing inlet and outlet ports to allow for adequate rinsing. Rinses utilized anhydrous toluene (Sigma–Aldrich, 99.8%) and uninhibited THF (Optima, Fisher Scientific). Fluorescein isothiocyanate (FITC) (Sigma–Aldrich, F2502) and 490 nm silica microspheres (Duke Scientific #8050) were used in the gel wall permeability study. LSCM images were taken on a Leica DMIRBE microscope with an SP-2 scan head equipped with an oil-immersion objective lens (63× plan-apochromat, NA 1.32) and

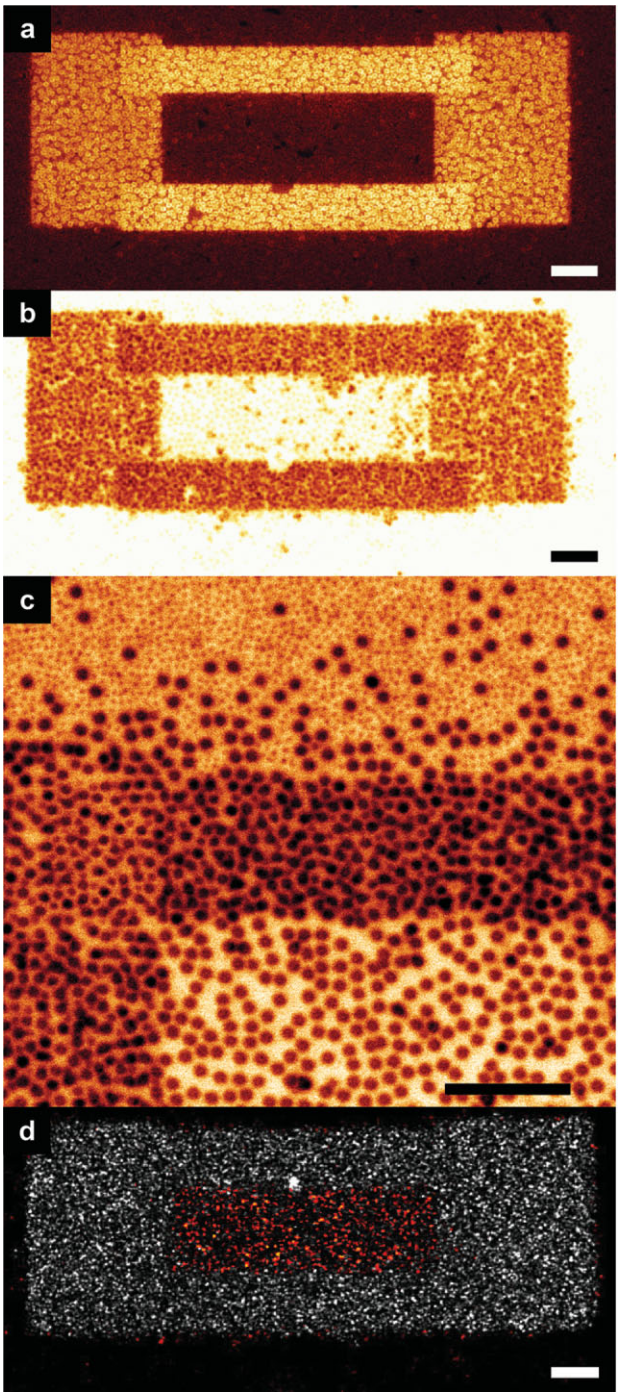

Figure 4. Confocal microscopy *x*–*y* sections of capped, porous-walled 3D microtubes. a) Fluorescence-mode section taken through cavity. Only the switched particles (MC form) are visible. b) The same structure after introduction of a fluorescent dye. c) Fluorescence-mode section taken at base of the cavity after introduction of 490 nm diameter silica colloids. d) Microcavity with trapped colloidal fluid. The moving particles are depicted in red, while the stationary particles (gel walls) are shown in grayscale. All scale bars = 10 μm.

Ar^+ and HeNe lasers. Multiphoton direct laser writing was achieved by coupling a Spectra-Physics Tsunami Ti/Sapphire laser with 10 W Spectra-Physics Millennia pump laser to the Leica SP-2 scan head. The bandwidth was approximately 10 nm, centered at 780 nm, and consisted of ~100 fs pulses with a repetition rate of 82 MHz. Laser power was modulated with a Linos Pulse Amplifier and electro-optical modulator (EOM) unit. Typical powers measured at the objective (Newport 1830-C power meter) varied from 36–40 mW for the high EOM setting and 0.30–0.34 mW for the low EOM setting. The LSCM operates in the standard fashion, where galvometer mirrors raster the laser (9.5 cm s^{-1}) in the lateral (*x*–*y*) dimensions through a square scan area in the focal plane of the objective. During each scan, the EOM modulates the laser beam between high and low settings in order to selectively expose a software-defined region of interest (ROI) within the scan area. By translating the sample in the transverse (*z*) dimension using a galvometer stage, 3D features with simple 2D cross-sections were fabricated. A combination of 2D ROIs written in series was used to rapidly fabricate the 3D microtubes and other structures. 3D reconstructions were rendered (AMIRA, Visage Imaging) using either the raw confocal volumetric image stack (Fig. 2f) or post-processed image stacks (Fig. 2c and i) as the input. For the latter case, the original volumetric image stacks were first analyzed (IDL, ITT Visual Information Solutions) to locate the particle centers via a local intensity maximum criterion. A new volumetric image stack was generated (MATLAB, The Mathworks) by placing a 1 μm diameter sphere at the (*x*, *y*, *z*) coordinates corresponding to each particle's center of brightness. This new image stack was then loaded into AMIRA for rendering. Figure 4d was generated (Adobe Photoshop CS2, Adobe Systems, Inc.) by comparing two confocal *x*–*y* slices from S2 of Supporting Information using Boolean operators. Pixels that changed from one image to the next were colored red and overlaid onto the unchanging pixels, shown in grayscale.

Direct Laser Writing: The sedimentation cell was assembled, filled halfway with anhydrous toluene, and mounted with the SP-*co*-MMA derivatized coverslip base in contact with the inverted LCSMs 63× oil objective. Dispersions (0.5–2.0 vol %) of 1 μm diameter SP-*co*- MMA-coated silica colloids were agitated in an ultrasonic bath in the dark for 5–20 min to break up any aggregates and ensure the colloids were in the sterically stabilized SP form. Approximately 2 mL of the colloidal dispersion was placed into the sedimentation cell, which was then sealed. After 5–10 min a thick colloidal sediment formed on top of the SP-*co*-MMA-derivatized coverslip. Multiphoton laser writing of the MRL gel structure started at the coverslip and proceeded 10 μm into the colloidal sediment. The self-supported mushroom structures were fabricated in a two-step process, starting at the coverslip with 8 μm diameter, 10 μm tall base followed by 24 μm diameter, and 6 μm tall mushroom cap. Multiphoton laser writing of the microtube structures proceeded from the coverslip by first patterning the channel walls. A 20 μm channel gap separated the colloidal gel walls, which were either 10 or 15 μm wide, 70 μm long, and 20 μm high. Next, the channel walls were covered by a 10 μm thick top that was exposed and re-exposed to improve structural integrity. Complications arising from the use of an elongated voxel (no beam expander, nonstandard coverslip), sample drift, and sedimentation/sagging of the channel-top resulted in a final thickness of ~15 μm. In another experiment, 5.5 μm wide, 20 μm high channel walls were fabricated with a 7 μm thick channel top, and a 5.5 μm channel gap (see Fig. S1 of Supporting Information). After phototriggered gelation of the desired features, the sedimentation cell was removed from the LSCM and agitated with flow into and out of a pipette, redispersing the ungelled sediment to yield a suspension of the microspheres (SP-form), which was replaced with anhydrous toluene. This agitation-rinsing process was repeated 3–4 additional times with toluene, and then 3–4 times with fresh, inhibitor-free THF, followed by two additional toluene rinses. The sedimentation cell with the gel-walled microstructures was then placed back on the LSCM for imaging and construction of end-caps (see Fig. 3b–e).

The microtube capping process began with multiphoton exposure of the ends of the existing open microtube structures. This ensures the microtube ends are in the aggregating MC state, so that photoresponsive colloids that come into contact with them are captured (and do not diffuse into the tube interior). The dispersion of SP-*co*-MMA-coated silica spheres was then reintroduced and after 1–2 min, the end caps were written, fusing the sedimenting colloidal species to the existing structure. The end caps had a

10 μm overlap with the microtube structures, resulting in 20 μm wide, 50 μm long, and 20 μm high cavity design rules. Rinsing with toluene and THF as before gave the desired microcavity structures. Reflectance-mode LSCM images were taken using the 633 nm HeNe line. Fluorescence-mode LSCM sections were taken after transfer into ethanol, using 488 nm Ar^+ laser excitation and an emission-detection window of 500–550 nm. FITC diluted in ethanol and several drops of the 2 wt% aqueous suspension of 490 nm silica microspheres were used to probe the permeability of the patterned colloidal features.

Acknowledgements

We thank Greg Jamison and Timothy Long for their work in developing the synthetic routes for the spirobenzopyran compounds, and Alex Jerez for helping prepare the 3D renderings in Maya. This work has been carried out within the Microscopy Suite and the Visualization, Imaging, and Media Laboratory at the Beckman Institute for Advanced Science and Technology at the University of Illinois at Urbana-Champaign (UIUC) and within Sandia National Laboratories, Albuquerque, New Mexico. The UIUC component of this work is supported by the US Department of Energy, Division of Materials Sciences, under Award no. DE-FG02-07ER46471, through the Frederick Seitz Materials Research Laboratory at UIUC. Sandia funding was derived from the Center for Integrated Nanotechnology (CINT) and Sandia National Laboratory LDRD Program. Sandia is a multiprogram laboratory operated by Sandia Corporation, a Lockheed Martin Company, for the United States Department of Energy's National Nuclear Security Administration under contract DE-AC04-94AL85000. Supporting Information is available online from Wiley InterScience or from the author.

Received: April 23, 2008
Revised: June 30, 2008
Published online: October 15, 2008

[1] S. Noda, N. Yamamoto, H. Kobayashi, M. Okano, K. Tomoda, *Appl. Phys. Lett.* **1999**, *75*, 905.
[2] P. Yao, G. Schneider, D. Prather, E. Wetzel, D. O'Brien, *Opt. Express* **2005**, *13*, 2370.
[3] M. Alvaro, J. F. Aaron, R. Shuvo, *J. Micromech. Microeng.* **2006**, *16*, 276.
[4] J. Zaumseil, M. A. Meitl, J. W. P. Hsu, B. R. Acharya, K. W. Baldwin, Y. L. Loo, J. A. Rogers, *Nano Lett.* **2003**, *3*, 1223.
[5] P. Dario, M. C. Carrozza, N. Croce, M. C. Montesi, M. Cocco, *J. Micromech. Microeng.* **1995**, *5*, 64.
[6] A. Bertsch, H. Lorenz, P. Renaud, *Sens. Actuat. A. Phys.* **1999**, *73*, 14.
[7] B. H. Cumpston, S. P. Ananthavel, S. Barlow, D. L. Dyer, J. E. Ehrlich, L. L. Erskine, A. A. Heikal, S. M. Kuebler, I. Y. S. Lee, D. McCord-Maughon, J. Qin, H. Rockel, M. Rumi, X.-L. Wu, S. R. Marder, J. W. Perry, *Nature* **1999**, *398*, 51.
[8] D. Xia, S. R. J. Brueck, *J. Vac. Sci. Technol. B. Microelectron. Nanometer Struct.* **2005**, *23*, 2694.
[9] D. Therriault, S. R. White, J. A. Lewis, *Nat. Mater.* **2003**, *2*, 265.
[10] S. Jeon, V. Malyarchuk, J. O. White, J. A. Rogers, *Nano Lett.* **2005**, *5*, 1351.
[11] S. Jeon, J.-U. Park, R. Cirelli, S. Yang, C. E. Heitzman, P. V. Braun, P. J. A. Kenis, J. A. Rogers, *PNAS* **2004**, *101*, 12428.
[12] H. D. Gesser, P. C. Goswami, *Chem. Rev.* **1989**, *89*, 765.
[13] J. E. Smay, G. M. Gratson, R. F. Shepherd, J. Cesarano, J. A. Lewis, *Adv. Mater.* **2002**, *14*, 1279.
[14] Q. Li, J. A. Lewis, *Adv. Mater.*, **2003**, *15*, 1639.
[15] M. Piech, N. S. Bell, *Macromolecules* **2006**, *39*, 915.
[16] N. S. Bell, M. Piech, *Langmuir* **2006**, *22*, 1420.
[17] M. Piech, M. C. George, N. S. Bell, P. V. Braun, *Langmuir* **2006**, *22*, 1379.
[18] E. Kim, Y. K. Choi, M. H. Lee, S. G. Han, S. R. Keum, The 4th International Conference on Electronic Materials (August 24–27, 1998, Cheju, Korea) **1999**, 35, S615.
[19] Y. S. Park, Y. Ito, Y. Imanishi, *Macromolecules* **1998**, *31*, 2606.
[20] A. K. Chibisov, H. Gorner, *J. Photochem. Photobiol. A. Chem.* **1997**, *105*, 261.
[21] M. W. Carsten Schomburg, Y. Rohlfing, G. Schulz-Ekloff, D. Wöhrle, *J. Mater. Chem.* **2001**, *11*, 2014.
[22] M. Q. Zhu, L. Zhu, J. J. Han, W. Wu, J. K. Hurst, A. D. Q. Li, *J. Am. Chem. Soc.* **2006**, *128*, 4303.
[23] S. A. Pruzinsky, P. V. Braun, *Adv. Funct. Mater.* **2005**, *15*, 1995.
[24] B. Kaehr, J. B. Shear, *J. Am. Chem. Soc.* **2007**, *129*, 1904.